Title

Molecular Mechanisms and New Treatment Paradigm for Atrial Fibrillation

Journal

Circulation Arrhythmia and Electrophysiology, 9(5)

ISSN

1941-3149

Authors

Sirish, Padmini

Li, Ning

Timofeyev, Valeriy

et al.

Publication Date

2016-05-01

DOI

10.1161/circep.115.003721

Peer reviewed

HHS Public Access

Author manuscript

Circ Arrhythm Electrophysiol. Author manuscript; available in PMC 2017 May 01.

Published in final edited form as:

Circ Arrhythm Electrophysiol. 2016 May ; 9(5): . doi:10.1161/CIRCEP.115.003721.

Molecular Mechanisms and New Treatment Paradigm for Atrial Fibrillation

Padmini Sirish, PhD[1], **Ning Li, PhD**[1], **Valeriy Timofeyev, PhD**[1], **Xiao-Dong Zhang, PhD**[1], **Lianguo Wang, MD**[2], **Jun Yang, PhD**[3], **Kin Sing S. Lee, PhD**[3], **Ahmed Bettaieb, PhD**[4], **Sin Mei Ma, BS**[1], **Jeong Han Lee, PhD**[5], **Demetria Su, BS**[1], **Victor C. Lau, BS**[1], **Richard E. Myers, PhD**[1], **Deborah K. Lieu, PhD**[1], **Javier E. López, MD**[1], **J. Nilas Young, MD**[6], **Ebenezer N. Yamoah, PhD**[5], **Fawaz Haj, PhD**[4], **Crystal M. Ripplinger, PhD**[2], **Bruce D. Hammock, PhD**[3], and **Nipavan Chiamvimonvat, MD**[1,7]

[1]Division of Cardiovascular Medicine, University of California, Davis

[2]Department of Pharmacology, University of California, Davis

[3]Department of Entomology and Nematology and Comprehensive Cancer Center, University of California, Davis

[4]Department of Nutrition, University of California, Davis

[5]Department of Physiology and Cell Biology, University of Nevada, Reno

[6]Department of Cardiothoracic Surgery, University of California, Davis

[7]Department of Veterans Affairs, Northern California Health Care System, Mather, CA

Abstract

Background—Atrial fibrillation (AF) represents the most common arrhythmia leading to increased morbidity and mortality, yet, current treatment strategies have proven inadequate. Conventional treatment with antiarrhythmic drugs carries a high risk for proarrhythmias. The soluble epoxide hydrolase enzyme (sEH) catalyzes the hydrolysis of anti-inflammatory epoxy fatty acids including epoxyeicosatrienoic acids (EETs) from arachidonic acid to the corresponding pro-inflammatory diols. Therefore, the goal of the study is to directly test the hypotheses that inhibition of the sEH enzyme can result in an increase in the levels of EETs leading to the attenuation of atrial structural and electrical remodeling and the prevention of AF.

Methods and Results—For the first time, we report findings that inhibition of sEH reduces inflammation, oxidative stress, atrial structural and electrical remodeling. Treatment with sEH inhibitor significantly reduces the activation of key inflammatory signaling molecules, including the transcription factor nuclear factor κ-light-chain-enhancer (NF-κB), mitogen-activated protein kinase (MAPK) and transforming growth factor-β (TGF-β).

Correspondence: Nipavan Chiamvimonvat, Division of Cardiovascular Medicine, University of California, Davis, 451 Health Science Drive, GBSF 6315, Davis, CA 95616, Tel: 530-754-7158, Fax: 530-754-7167, nchiamvimonvat@ucdavis.edu.

Disclosure: B.D.H. and N.C. have filed patents for the use of sEH inhibitors in cardiomyopathy and arrhythmias.

Conclusions—This study provides insights into the underlying molecular mechanisms leading to AF by inflammation and represents a paradigm shift from conventional antiarrhythmic drugs which block downstream events to a novel upstream therapeutic target by counteracting the inflammatory processes in AF.

Keywords

arrhythmia; atrial fibrillation; inflammation; animal model; eicosanoids; soluble epoxide hydrolase inhibitors; Fibrosis

Introduction

Atrial fibrillation (AF) represents one of the most common arrhythmias seen clinically and is associated with a significant increase in morbidity and mortality[1], yet, current treatment paradigms have proven largely inadequate.[2] Treatment with conventional antiarrhythmic drugs generally carries a high risk of proarrhythmia.[3] Moreover, prevalence of AF is increasing due to the aging population.

There is strong evidence supporting the involvement of inflammation in the pathophysiology of AF.[1,4,5] Inflammatory infiltrates and increased serum levels of proinflammatory cytokines have been demonstrated in animal models and patients with AF.[6–8] In addition, inflammation has been implicated in diseases which predispose patients to AF and AF-related processes including oxidative stress and fibrosis.[5,7] Structural and electrical remodeling represents the main pathophysiological mechanisms contributing to the initiation and maintenance of AF. Moreover, AF can exacerbate inflammation which further perpetuates the arrhythmia. Hence, reduction of inflammation and reversal of structural remodeling have increasingly become the focus of new therapeutic strategies for the treatment of AF.

One of the most robust inflammatory responses is the activation of phospholipase A_2 and the release of arachidonic acid, which is metabolized through the cyclooxygenase (COX), lipoxygenase (LOX), and cytochrome P450 (CYP450) pathways. The CYP450 epoxidized products, the epoxyeicosatrienoic acids (EETs) have been shown to have anti-inflammatory and pro-fibrinolytic with several cardioprotective effects.[9] However, EETs are further metabolized by the soluble epoxide hydrolase (sEH) enzyme to form the corresponding 1,2-diols, dihydroxyeicosatrienoic acids (DHETs) with diminished anti-inflammatory activities.[9] Indeed, the cardioprotective activity of EETs can be enhanced by blocking the degradation of EETs to corresponding DHETs using novel inhibitors of sEH (sEHI).[10] We have previously demonstrated the beneficial effects of sEHIs in clinically relevant models of cardiac hypertrophy and failure.[11–14] We further demonstrate that treatment with sEHIs reduces atrial arrhythmia inducibility in cardiac hypertrophy models.[12] However, the molecular mechanisms underlying the prevention of atrial arrhythmia inducibility by sEHIs remain unexplored.

Hence, in the current study, we sought to directly test the molecular mechanisms in the prevention of AF using an *in vivo* pressure-overload model to replicate chronic hypertension, a major risk factor for AF. We further utilize an *in vitro* model of human-

induced pluripotent stem cell (hiPSC)-derived atrial myocytes and fibroblasts to test the hypotheses that inhibition of sEH attenuates AF by reducing 1) inflammation, 2) atrial structural remodeling, and 3) electrical remodeling in atrial myocytes. Our study not only provides important mechanistic insights into the roles of inflammation and atrial fibrosis in AF but also represents a proof-of-concept study for a novel therapeutic target for the treatment of AF.

Methods

The animal study was performed in accordance with the approved UC Davis Animal Care and Use protocol. Additional experimental details can be found in the Supplemental Methods.

Thoracic Aortic Constriction (TAC) model in mice

TACs were performed in 8- to 12-week-old male C57BL/6J mice as previously described.[13] One week after surgery, mice were randomized in an investigator-blinded manner to receive either vehicle alone or 1-Trifluoromethoxyphenyl-3-(1-Propionylpiperidine-4-yl)Urea (TPPU, Fig. 1a) for three weeks (Fig. 1b).[13]

Analysis of cardiac function by echocardiography

Echocardiograms were performed as described previously.[12] Fractional shortening (FS) was calculated from left ventricle dimensions as follows: %FS = ((EDD−ESD)/EDD) ×100, where EDD and ESD represent end-diastolic and end-systolic dimensions, respectively.

Histological analyses

Excised hearts were retrogradely perfused with phosphate-buffered solution to wash out blood. Fixed hearts were embedded in paraffin, serial left atrial (LA) and right atrial (RA) sections of 5 μm in thickness were taken along the longitudinal axis and stained with Picrosirius Red to assess for collagen content.

Immunofluorescence confocal laser scanning microscopy

Additional cardiac sections were stained with wheat germ agglutinin (WGA). Deparaffinized sections were rehydrated with serial dilution of ethanol, serum blocked and stained. Sections from corresponding area from the four groups were scanned.

Flow cytometric and Electrophysiological studies of single isolated cardiac cells

Single cells were obtained using enzymatic digestion. LA and RA myocytes were utilized for electrophysiological studies using conventional whole-cell patch-clamp technique at room temperature.[12] Currents were recorded using Axopatch 200B amplifier, filtered at 10 kHz, and digitized at sampling frequency of 50 kHz.

For flow cytometric analysis, fixed cells were permeabilized, stained with anti-Thy1.2, lineage, anti-CD45, anti-troponin T, anti-CD31, anti-pERK1/2, anti-pSMAD2/3, Ki67 antibodies and 7-amino-actinomycin D (7-AAD). Data were collected using FACScan

cytometer and analyzed using FlowJo software. Cells stained with isotype-matched IgG antibodies were used as controls to determine the positive cell population.

Human-induced pluripotent stem cell-derived cardiomyocytes (hiPSC-CM)

HiPSC were plated and differentiated for 20 days using a directed differentiation protocol.[15] HiPSC-CMs enriched with puromycin and treated with Tumor Necrosis Factor-α (TNF-α) or Angiotensin II (ANG II) and TPPU were fixed and stained with anti-α-actinin, anti-NF-κB, anti-myosin light chain-2a (MLC2a), anti- myosin light chain-2v (MLC2v) and fibroblast-specific antibodies.

In vitro human cardiac fibroblast culture

Human right atrial appendage specimens from informed consented patients undergoing cardiac bypass surgery were obtained from UC Davis Medical Center in accordance with the approved UC Davis Institutional Review Board protocol. Partially digested cardiac tissues were plated on cell culture dishes until the appearance of fibroblasts from the explants. Trypsinized cells were re-plated, treated with ANG II and TPPU and stained with anti-Thy1.1, lineage, anti-CD45 and Ki67 antibodies for flow cytometry.

Western Blot Analysis

Immunoblots were performed as previously described[16] using anti-IκB, anti-phospho-IκB, anti-NF-κB and anti-GAPDH antibodies.

Measurement of Plasma Cytokine Levels

Plasma cytokine levels from samples collected 3 weeks after sham or TAC operation were analyzed using a Cytometric Bead Array kit and Cytometric Bead Array Analysis software following the manufacturers protocol.[13]

Evaluation of Endoplasmic Reticulum Stress markers

Total protein isolated from atrial tissues homogenized in RIPA buffer supplemented with protease and phosphatase inhibitors were resolved by SDS-PAGE and immunoblotting was performed using antibodies for pp38 (Thr180/Tyr182), p38, pJNK (Thr183/Tyr185), JNK, pPERK (Thr980), PERK, peIF2α (Ser51), eIF2α, sXBP1, IRE1α, pIRE1α (Ser724) and Tubulin. Proteins were visualized using enhanced chemiluminescence and quantified using ImageQuant 5.0 software. Data for phosphorylated proteins are presented as phosphorylation level normalized to total protein expression and for non-phosphorylated proteins as total protein expression normalized to β-tubulin.

Ex vivo Optical Mapping of transmembrane potential (V_m)

Hearts from heparin-injected anesthetized mice were perfused in Tyrode's solution with the posterior surface of the heart facing the optical mapping camera using Langendorff apparatus.[17] A bipolar pacing electrode was positioned on the epicardium of left or right atrial appendage for pacing using a 2 ms pulse at twice the diastolic threshold. The heart was stained with the voltage-sensitive dye (RH237) via the coronary perfusion. Optical action

potentials were recorded using a 16-bit complementary metal oxide camera and images acquired at 1 kHz.

Statistical Analysis

Statistical comparisons were analyzed by one-way ANOVA followed by Bonferroni tests and Tukey's-Kramer honest significant difference analyses for post hoc comparison.

Results

Prevention of atrial myocyte hypertrophy with sEHI in a murine TAC model

TPPU has been shown previously to have high inhibitory potency, long enzyme dissociation half-life, pharmacokinetic half-life with drug-like properties and a comparable elevation of EETs concentration in plasma as the *sEH* knockout mice (*EPHX2*$^{-/-}$).[13,18] TAC mice exhibited cardiac hypertrophy, a significant increase in heart weight to body weight ratio (HW/BW Figs. 1c and d) and atrial dilation (Fig S1a and b). In contrast, treatment with TPPU in TAC mice resulted in a decrease in HW/BW ratio and atrial dilatation. Flow cytometry confirmed the presence of the sEH enzyme in the atrial myocytes (Fig. S1c).

We analyzed the forward light scattering by flow cytometry as an index of atrial myocyte size using isolated single atrial cells. Atrial myocytes were gated based on the presence of cardiac-specific troponin T. There was a significant increase in atrial myocyte size in TAC-operated group (Figs. 1e and f) compared to sham-operated groups. More importantly, atrial myocyte hypertrophy was reduced in animals treated with TPPU (Fig. 1f). We further confirmed the findings using patch-clamp recordings and cell capacitance measurement showing a significant increase in myocyte size in TAC-operated mice (118±4 pF) compared to sham, sham-operated and TAC-TPPU treated groups (64±10, 67±7, and 71±2 pF, respectively). Finally, the myocyte size from LA and RA was directly compared using a Coulter multisizer assay to quantify the cell volume.[13] The myocyte volume significantly increased in both LA and RA from TAC mice, which was restored to the sham-operated control levels by the TPPU treatment (Fig. 1g). Interestingly, the myocyte volume was significantly smaller for RA compared to LA in all three groups (sham, TAC, and treated-TAC, $p<0.05$).

The effect of TPPU on the chamber size and systolic function was assessed using echocardiography. There was a significant decrease in left-ventricular end diastolic dimension (LVEDD, Fig. S2) associated with a significant improvement in fractional shortening (FS, Fig. 1h) post TPPU treatment. In contrast, LVEDD in TAC mice increased from week one to week four suggesting adverse remodeling.

Target engagement of TPPU in mouse TAC model

To demonstrate the inhibition of sEH by TPPU, metabolic profiling of arachidonic acid (AA) metabolites of the *CYP450* pathway was performed after three weeks of treatment as previously described.[13] There was a significant increase in the EETs/DHETs ratio in the TPPU-treated groups compared with TAC alone group (Fig. 1i and Table S1). Moreover, analysis of AA metabolites of the *COX* pathway demonstrates an increase in

proinflammatory thromboxane and prostaglandin levels in the TAC model which was attenuated with TPPU treatment (Fig. S3a and Table S2). Metabolites of the *LOX* pathways demonstrated a modest difference between the four groups (Fig. S3b and Table S2).

Treatment with TPPU results in a significant reduction in inflammatory cytokines and chemokine

Although the precise underlying mechanisms for atrial fibrosis in AF have not been fully elucidated, a network of profibrotic factors including proinflammatory cytokines is known to contribute towards AF in the clinical setting.[19] Our data demonstrates a significant increase in proinflammatory cytokine and chemokine levels including interferon-γ (IFN-γ), TNF-α, and monocyte chemoattractant protein-1 (MCP-1) in the TAC mice (Figs. 1j and k) in TAC animals. Importantly, treatment with TPPU significantly decreased the cytokine and chemokine levels.

Treatment with TPPU significantly reduces atrial fibrosis and atrial fibroblast activation

Previous studies have provided a strong link between atrial fibrosis and atrial structural remodeling in the development of AF,[1,4] however, the precise mechanisms for atrial fibrosis remain incompletely understood. The secretory, migratory, and proliferative capacity of cardiac fibroblasts increases after injury.[13] Proinflammatory cytokines and profibrotic factors such as ANG II induce cardiac fibrosis by activating cardiac fibroblasts resulting in an increase in collagen synthesis.[1] However, there are regional differences in structural remodeling between atria and ventricles with atria being particularly prone to fibrosis.[20] Indeed, atrial fibroblasts are distinct from ventricular fibroblasts in their morphology, gene expression, secretory, and proliferative patterns.[21]

Here, we demonstrate the presence of atrial fibrosis in LA (Figs. 2a and b) and RA (Fig. S4) sections using Picrosirius Red stain and wheat germ agglutinin that binds to highly glycosylated collagen protein in TAC hearts. However, there was a marked decrease in collagen deposition in the TPPU-treated atrial tissue sections compared to the TAC alone. Next, we analyzed atrial fibroblasts isolated from sham, sham-treated, TAC and TAC-treated hearts. Atrial fibroblasts were defined as $Thy1.2^{+}/Lin^{-}/CD31^{-}/CD45^{-}$ cells (Mouse-Thy^{pos} cells) using flow cytometry.[13] There was a significant increase in percentages of Thy^{pos} cells in the atria of TAC compared to the two groups of sham animals (Figs. 2c and d). Treatment with TPPU resulted in a significant decrease in percentages of Thy^{pos} cells compared to TAC animals.

In vitro models of human atrial fibroblasts and hiPSC-derived cardiac fibroblasts

The effects of TPPU observed in the atria may be secondary to the reduction in ventricular hypertrophy and adverse remodeling in the ventricles. Therefore, to directly demonstrate the effects of sEH inhibition specifically on atrial fibroblasts and independent of ventricular influence, we used atrial fibroblasts isolated from human atrial appendages as well as an *in vitro* model of hiPSC-derived cardiac fibroblasts (hiPSC-fibroblasts).

Human atrial fibroblasts were isolated and quantified as cells expressing $Thy1.1^{+}/Lin^{-}/CD45^{-}$ (Human-Thy^{pos} cells) using flow cytometry (Fig. 2e). There was a significant

increase in percentages of human atrial fibroblasts in the ANG II treated group compared to the control (Fig. 2f) and treatment with TPPU resulted in a decrease in percentages of human Thy^{pos} cells. We further utilized Ki67 to analyze the proliferative capacity among human atrial fibroblasts stimulated with ANG II. There was a significant increase in the percentage of Ki67 in the ANG II-treated human atrial fibroblasts compared to control (Figs. 2g and h). Treatment with TPPU in the ANG II stimulated cells resulted in a significant decrease in Ki67 positivity in the human atria fibroblasts.

HiPSC-fibroblasts were defined as $Thy1.1^{+}/Lin^{-}/CD45^{-}$ cells (hiPSC-Thy^{pos} cells). ANG II treatment significantly increased the percentages (Fig. 2i and j) and proliferative capacity (Figs. 2k and l) of hiPSC-fibroblasts compared to the control. Treatment with TPPU in the ANG II stimulated cells resulted in a significant decrease in the percentages and Ki67 positivity in the hiPSC-fibroblasts.

Treatment with TPPU results in a significant reduction in the activation of MAPK and TGF-β signaling cascades in atrial fibroblasts and myocytes

Inflammatory cytokines and chemokines including IFN-γ, TNF-α, and MCP-1 have been shown to contribute to cardiac fibrosis by activating cardiac fibroblasts *via* the mitogen-activated protein kinase (MAPK) signaling cascade.[13] Indeed, increased circulatory levels of TNF-α have been demonstrated in patients with heart failure.[22] The Smad signaling cascade regulated by transforming growth factor-β (TGF-β) also contributes to cardiac fibrosis.[23] Upregulated TGF-β in cardiac fibroblasts activates Smad transcription factors, which translocate to the nucleus to activate the promoters of collagen I and III genes.[24,25] Moreover, cardiac hypertrophy is also stimulated by the interplay of MAPK and TGF-β.[25,26]

To elucidate the effects of TPPU on the MAPK and TGF-β signaling cascades, we examined the activation of downstream members, the extracellular signal regulated kinase 1 and 2 (ERK1/2) and Smad2/3 in atrial fibroblasts and myocytes. Our data demonstrates a significant elevation in the levels of phosphorylated ERK1/2 (pERK1/2) in atrial fibroblasts (Figs. 3a and b) and myocytes (Figs. 3c and d) in the TAC mice that was significantly decreased in TPPU-treated TAC mice. Similarly, there was a significant elevation in the levels of phosphorylated Smad2/3 (Smad2/3) in atrial fibroblasts (Figs. 3e and f) and myocytes (Figs. 3g and h) in the TAC mice that was significantly decreased in TPPU-treated TAC mice. Taken together, our data suggest that TPPU decreases the production of cytokines and chemokines resulting in the decrease in the activation of atrial fibroblasts and myocyte hypertrophy, the leading contributors of adverse atrial structural remodeling associated with AF.

Treatment with TPPU results in a significant reduction in oxidative stress in atrial fibroblasts and myocytes

Systemic and myocardial-specific oxidative stress has been implicated in the pathogenesis of AF.[27] Elevated systemic levels of reactive oxygen species (ROS) are seen with increasing age, heart failure, and coronary heart disease which are known risk factors for AF.[28] Here, flow cytometry was used to quantify the level of oxidative stress in atrial fibroblasts (Figs. 3i and j) and atrial myocytes (Figs. 3k and l). There was a significant increase in ROS levels in

atrial fibroblasts and atrial myocytes isolated from TAC compared to the two groups of sham animals. Moreover, treatment with TPPU resulted in a significant decrease in the ROS activity compared to TAC alone.

Direct effects of TPPU in an in vitro model of hiPSC-derived atrial myocytes and fibroblasts activated by inflammatory cytokine TNF-α

As mentioned above, the effects of sEHI in the prevention of atrial remodeling may be secondary to the reduction in ventricular hypertrophy. Therefore, to specifically elucidate the effects of inflammatory cytokines and the direct inhibitory effects of TPPU on atria, we used an *in vitro* model of hiPSC-derived atrial myocytes (hiPSC-ACMs) and hiPSC-fibroblasts. HiPSC-ACMs were selected based on the expression of MLC2a and the absence of MLC2v (Figs. 4a and b).[29] Differentiated-hiPSCs were treated with TNF-α. Analysis of hiPSC-ACMs ($MLC2a^{+}/MLC2v^{-}$) and hiPSC-fibroblasts stimulated with TNF-α demonstrated a significant increase in pERK1/2 compared to the control and control-TPPU treated cells (Figs. 4c–e). Moreover, treatment of TNF-α stimulated hiPSC-ACMs and hiPSC-fibroblasts with TPPU significantly decreased the pERK1/2 level. The presence of the sEH enzyme in hiPSCs was analyzed by flow cytometry (Fig. 4f).

Treatment with TPPU results in a significant reduction in the activation of the nuclear factor κ-light-chain-enhancer of activated B cells (NF-κB)

NF-κB represents one of the critical players in the cytokine-mediated inflammation and is associated with cardiac fibrosis, hypertrophy, and heart failure.[9] NF-κB is maintained in the inactive form when bound to IκB. Degradation of IκB by IκB kinase leads to the nuclear translocation of NF-κB and gene activation. EETs have been shown to regulate the NF-κB cascade by inhibiting IκB kinase.[9] Our data demonstrated an increased nuclear translocation of NF-κB in hiPSC-CM (Fig. 5a) and a significant increase in the pIκBα and nuclear NF-κB (nNF-κB) upon TNF-α stimulation, which was significantly attenuated with TPPU treatment (Figs. 5b–d).

Treatment with TPPU results in a significant reduction in Endoplasmic Reticulum (ER) Stress

Increasing evidence suggests that ER stress contributes to cardiac hypertrophy, fibrosis, and apoptosis.[30,31] Perturbations in the ER homeostasis due to intrinsic and extrinsic factors such as inflammation, oxidative stress, and ischemia may culminate in ER stress. This includes the activation of ER transmembrane protein sensors (PKR-like ER-regulated kinase (PERK) and inositol requiring enzyme 1α (IRE1α)), the up-regulation of ER chaperones such as binding of immunoglobulin protein (BIP), initiation of ER-related apoptotic proteins such as CCAAT/enhancer-binding protein homologous protein (CHOP), and activation of MAPKs.[32–34]

Chronic pressure overload in TAC animals resulted in the activation of PERK and IRE1α, and their downstream targets α-subunit of eukaryotic translation initiation factor 2 (eIF2α) and X-box binding protein 1 (XBP1), respectively in atrial tissues (Fig. S5a). Treatment with TPPU significantly attenuated ER stress in atrial tissues as evidenced by decreased PERK (Thr980), eIF2α (Ser51) and IRE1α (Ser724) phosphorylation, decreased XBP1 splicing

expression, and a decrease in BIP and CHOP compared to TAC mice (Figs. S5b–g). Since the activation of MAPKs constitutes a component of the stress response in atrial hypertrophy[35] and plays an important role in mediating signal transduction from the ER to the cell nucleus, we evaluated activation of MAPKs. Notably, TAC-induced phosphorylation of p38 (Thr180/Tyr182) and c-Jun N-terminal kinases (JNK, Thr183/Tyr185) was lower in TPPU-treated TAC mice (Figs. S5h and i). The β-tubulin levels remain unchanged in the four groups (Fig S5j).

Treatment with TPPU reduces atrial electrical remodeling

Finally, optical mapping of transmembrane potential (V_m) was performed on isolated atria to determine the effects of TPPU on atrial electrical remodeling.[36] There was an increase in action potential duration (APD, Figs. 6a–d) in the atria isolated from TAC compared to TPPU-treated TAC animals. Atria from TAC hearts demonstrated a significant increase in APD at 80% of repolarization (APD_{80}) and APD dispersion (differences between LA and RA APD) compared to the TPPU-treated atria. Furthermore, atria isolated from TAC mice showed significantly longer effective refractory period (ERP) in the LA *vs.* RA (Fig. 6e) indicating increased dispersion of repolarization and refractoriness in untreated hearts.

Consistent with the *ex vivo* findings, patch-clamp recordings from single isolated atrial myocytes demonstrated a significant down-regulation of the transient outward K^+ current in TAC animals compared to sham or treated sham animals. Treatment with TPPU prevented the down-regulation of the transient outward K^+ current (Figs. 6f and g).

Discussion

Chronic hypertension represents one of most common co-morbidities leading to AF.[37] The main pathophysiological mechanisms contributing to the initiation, progression and persistence of AF are structural and electrical remodeling of the atria.[37] Moreover, AF increases inflammation in the heart contributing to atrial remodeling substantiating the ‘AF begets AF’ phenomenon.[7] In the present study, we provide a proof-of-concept and molecular mechanisms underlying the beneficial effects of inhibition of sEH in the treatment of AF. We demonstrate positive effects of sEHI in a pressure-overload-induced atrial remodeling model by reducing 1) inflammation, 2) atrial fibrosis, and 3) electrical remodeling in atrial myocytes. Specifically, the current study provides evidence to support the role of inhibition of sEH as a potent anti-inflammatory mechanism leading to a significant decrease in the systemic levels of cytokines and chemokines as well as the inhibition of NF-κB activation. Moreover, treatment with sEHI results in significant attenuation in the phosphorylation of key signaling molecules including ERK1/2 in the MAPK pathway in atrial myocytes and atrial fibroblasts. To further demonstrate direct inhibitory effects of sEHI on atrial myocytes and atrial fibroblasts, we took advantage of *in vitro* models of hiPSC-ACMs and hiPSC-fibroblasts as well as human atrial fibroblasts isolated from atrial appendages. Taken together, our data provide compelling molecular and cellular evidence for the use of sEHI as an anti-inflammatory therapy for AF (Fig. 6h).

Roles of inflammation in AF

Inflammation has been shown to play critical roles in the pathophysiology of AF.[8] Evidence of inflammatory infiltrates and increased serum levels of proinflammatory cytokines were present in both animal models and patients with AF.[6–8] Several important molecular mediators in inflammatory responses in AF include the stretch-activated production of ANG II and the recruitment of inflammatory cells that secrete inflammatory cytokines and chemokines that activate one of the critical transcription factor, NF-κB. Activated NF-κB not only increases the gene expression of inflammatory cytokines, intensifying inflammation, it also leads to electrical remodeling and myocytes hypertrophy. Hence, inflammatory cytokines act *via* a positive feedback mechanism further exacerbating AF (Fig. 6h).

Inflammatory cytokines such as TNF-α and INF-γ also disrupt protein folding in the ER. The ER is a multifunctional organelle playing an important role in protein-folding, calcium homeostasis and in particularly in the heart it also contributes to the regulation of excitation-contraction coupling.[32,34] When the folding capacity of ER is exceeded, misfolded proteins accumulate triggering ER stress. To mitigate ER stress and to restore ER homeostasis, the unfolded protein response (UPR) is initiated. However, if UPR mechanisms are unable to lessen ER stress, cardiomyocyte apoptosis occurs which contributes to the development and maintenance of AF.[38] In addition, ER stress induced apoptosis is initiated *via* the activation of NF-κB.[34]. Our data demonstrates a significant attenuation in the ER stress proteins with TPPU treatment. The *in vitro* data also demonstrates a decrease in the activation of NF-κB with TPPU treatment. Taken together, our data suggest that treatment with TPPU decreases ER stress at least in part through the inhibition of NF-κB activation.

Atrial structural remodeling and AF

AF-induced structural remodeling is a gradual process that intensifies progressively. Excessive oxidative stress has been associated with AF leading to atrial structural remodeling including atrial myocyte hypertrophy and fibrosis.[27,28] Experimental animal models and clinical studies have implicated multifactorial processes including atrial dilatation, cellular hypertrophy, apoptosis, ER stress, fibrosis, and oxidative stress as contributing to structural remodeling.[27,30] Increased fibrosis initiated by pro-fibrotic cytokines such as TGF-β1 has been observed in AF patients.[1,4,21] Atrial fibrosis has been shown to involve a complex interplay of profibrotic molecules including angiotensin II and its downstream mediators, the multifunctional MAPKs and TGF-β.[13,24,25] Upregulated TGF-β in cardiac fibroblasts induces cardiac fibrosis by activating Smad transcription factors, which activate the promoters of collagen I and III genes.[24,25] TGF-β also promotes persistent perivascular and interstitial fibrosis by suppressing the activity of matrix metalloproteinases and protease inhibitors.[13,25]

Atrial myocyte hypertrophy further increases ROS production in the atrial myocytes resulting in the activation of programmed cell death and apoptosis. Increased ROS production in cardiomyocytes causes the activation of members of the MAPK pathway, ERK1/2 and JNKs, both of which have been implicated in cardiac hypertrophy.[39] Similarly,

members of the pleiotropic TGF-β superfamily have been shown to promote myocardial hypertrophy.[25,26]

Here, we demonstrate an increase in both atrial fibrosis and atrial myocyte hypertrophy in the chronic pressure overload model, which is significantly mitigated by treatment with sEHIs. Treatment with sEHI significantly decreases the activation of ERK1/2 and Smad2/3 in atrial fibroblasts and myocytes. Inhibition of sEH attenuates ROS in atrial myocytes and fibroblasts by preventing the activation of the MAPK pathway, ERK1/2 and JNK. Moreover, sEHI decreases ER stress consistent with previous findings of the reduction of ER stress response in various disease models by sEH inhibition.[32,33] Finally, direct effects of sEHI on atrial myocytes and fibroblasts are further substantiated using *in vitro* model of hiPSC-fibroblasts and hiPSC-ACMs.

Atrial electrical remodeling and AF

Electrical remodeling is induced by rapid atrial rates, which develops immediately following AF and contributes to the stability of a longer lasting form of AF. Abnormalities in electrical impulse formation or impulse conduction can initiate and maintain AF. Excessive prolongation of APD causes Ca^{2+} currents to recover from inactivation leading to early after depolarization and maintenance of AF.[40] Our study demonstrates a slowing of activation, a prolonged APD in LA, and importantly an increased dispersion of APD and ERP, a known pro-arrhythmic factor. At the cellular basis, electrical remodeling involves changes to the ion channels governing the AP characteristics. Down-regulation of I_{to} in atrial cells can significantly alter AP shape and duration contributing to electrical remodeling. A marked decrease in I_{to} was previously documented in both animal models and chronic AF patients.[41] The reduction in I_{to} has been shown to be due to the decrease in the auxiliary subunit of the K^+ channel thereby impairing the channel assembly *via* the activation of NF-κB signaling cascade.[42]

SEH inhibition increases EETs, which has previously been shown to regulate gene expression *via* the inhibition of NF-κB signaling.[9,14] Of considerable relevance are our findings that there is a significant up-regulation of I_{to} from single isolated atrial myocytes and an inhibition of NF-κB activation in cultured cells by treatment with sEHI. Taken together, our data support the notion that treatment with sEHI may reduce the electrical remodeling in the atrial myocytes by the up-regulation of outward transient K^+ current, possibly through the inhibition of the NF-κB activation.

Translational Implications

The emergence of hiPSC technology has created a unique tool to study the effects of various drugs in both monogenetic diseases and in diseases with multiple etiologies such as AF. Advantages of using hiPSC for drug screening include the ability to circumvent the problem of maintaining primary human cardiomyocytes in culture, the ability to obtain patient-specific cell lines and the ability to avoid adverse side effects of drugs.[43] In our study, we took advantage of hiPSC-cardiomyocytes as a model system to study the effects of novel sEHI on the molecular mechanisms underlying the structural and electrical remodeling in AF. Indeed, hiPSC-ACMs may be utilized as an *in vitro* drug-screening tool to study atrial

arrhythmias. Finally, our study provides a proof-of-concept study for an upstream therapeutic target for the treatment of AF.

Supplementary Material

Refer to Web version on PubMed Central for supplementary material.

Acknowledgments

Funding Sources: Supported by NIH (R01 HL085727, R01 HL085844 and S10 RR033106 to NC), VA Merit Review Grant I01 BX000576 (to NC), American Heart Association Beginning Grant-in-Aid (to XZ), and American Heart Association Predoctoral Fellowship Award (to PS). PS received Postdoctoral Fellowship from California Institute for Regenerative Medicine (CIRM) Training Grant to UC Davis and NIH/NHLBI Institutional Training Grant in Basic and Translational Cardiovascular Science (T32 NIH HL086350). NC is the holder of the Roger Tatarian Endowed Professor in Cardiovascular Medicine.

References

1. Burstein B, Nattel S. Atrial fibrosis: mechanisms and clinical relevance in atrial fibrillation. J Am Coll Cardiol. 2008; 51:802–809. [PubMed: 18294563]
2. Wilton SB, Fundytus A, Ghali WA, Veenhuyzen GD, Quinn FR, Mitchell LB, Hill MD, Faris P, Exner DV. Meta-analysis of the effectiveness and safety of catheter ablation of atrial fibrillation in patients with versus without left ventricular systolic dysfunction. Am J Cardiol. 2010; 106:1284–1291. [PubMed: 21029825]
3. Akiyama T, Pawitan Y, Greenberg H, Kuo CS, Reynolds-Haertle RA. Increased risk of death and cardiac arrest from encainide and flecainide in patients after non-Q-wave acute MI in the Cardiac Arrhythmia Suppression Trial. Am J Cardiol. 1991; 68:1551–1555. [PubMed: 1720917]
4. Everett TH 4th, Olgin JE. Atrial fibrosis and the mechanisms of atrial fibrillation. Heart Rhythm. 2007; 4:S24–27. [PubMed: 17336879]
5. Guo Y, Lip GY, Apostolakis S. Inflammation in atrial fibrillation. J Am Coll Cardiol. 2012; 60:2263–2270. [PubMed: 23194937]
6. Sun M, Chen M, Dawood F, Zurawska U, Li JY, Parker T, Kassiri Z, Kirshenbaum LA, Arnold M, Khokha R, Liu PP. Tumor necrosis factor-alpha mediates cardiac remodeling and ventricular dysfunction after pressure overload state. Circulation. 2007; 115:1398–1407. [PubMed: 17353445]
7. Harada M, Van Wagoner DR, Nattel S. Role of inflammation in atrial fibrillation pathophysiology and management. Circ J. 2015; 79:495–502. [PubMed: 25746525]
8. Corradi D, Callegari S, Maestri R, Benussi S, Alfieri O. Structural remodeling in atrial fibrillation. Nat Clin Pract Cardiovasc Med. 2008; 5:782–796. [PubMed: 18852714]
9. Spector AA, Fang X, Snyder GD, Weintraub NL. Epoxyeicosatrienoic acids (EETs): metabolism and biochemical function. Prog Lipid Res. 2004; 43:55–90. [PubMed: 14636671]
10. Morisseau C, Hammock BD. Epoxide hydrolases: mechanisms, inhibitor designs, and biological roles. Annu Rev Pharmacol Toxicol. 2005; 45:311–333. [PubMed: 15822179]
11. Li N, Liu JY, Qiu H, Harris TR, Sirish P, Hammock BD, Chiamvimonvat N. Use of metabolomic profiling in the study of arachidonic acid metabolism in cardiovascular disease. Congest Heart Fail. 2011; 17:42–46. [PubMed: 21272227]
12. Li N, Liu JY, Timofeyev V, Qiu H, Hwang SH, Tuteja D, Lu L, Yang J, Mochida H, Low R, Hammock BD, Chiamvimonvat N. Beneficial effects of soluble epoxide hydrolase inhibitors in myocardial infarction model: Insight gained using metabolomic approaches. J Mol Cell Cardiol. 2009; 47:835–845. [PubMed: 19716829]
13. Sirish P, Li N, Liu JY, Lee KS, Hwang SH, Qiu H, Zhao C, Ma SM, López JE, Hammock BD, Chiamvimonvat N. Unique mechanistic insights into the beneficial effects of soluble epoxide hydrolase inhibitors in the prevention of cardiac fibrosis. Proc Natl Acad Sci U S A. 2013; 110:5618–5623. [PubMed: 23493561]

14. Xu D, Li N, He Y, Timofeyev V, Lu L, Tsai HJ, Kim IH, Tuteja D, Mateo RK, Singapuri A, Davis BB, Low R, Hammock BD, Chiamvimonvat N. Prevention and reversal of cardiac hypertrophy by soluble epoxide hydrolase inhibitors. Proc Natl Acad Sci U S A. 2006; 103:18733–18738. [PubMed: 17130447]
15. Lian X, Zhang J, Azarin SM, Zhu K, Hazeltine LB, Bao X, Hsiao C, Kamp TJ, Palecek SP. Directed cardiomyocyte differentiation from human pluripotent stem cells by modulating Wnt/beta-catenin signaling under fully defined conditions. Nat Protoc. 2013; 8:162–175. [PubMed: 23257984]
16. Sirish P, López JE, Li N, Wong A, Timofeyev V, Young JN, Majdi M, Li RA, Chen HS, Chiamvimonvat N. MicroRNA profiling predicts a variance in the proliferative potential of cardiac progenitor cells derived from neonatal and adult murine hearts. J Mol Cell Cardiol. 2012; 52:264–272. [PubMed: 22062954]
17. De Jesus NM, Wang L, Herren AW, Wang J, Shenasa F, Bers DM, Lindsey ML, Ripplinger CM. Atherosclerosis exacerbates arrhythmia following MI: Role of myocardial inflammation. Heart Rhythm. 2015; 12:169–178. [PubMed: 25304682]
18. Li L, Li N, Pang W, Zhang X, Hammock BD, Ai D, Zhu Y. Opposite effects of gene deficiency and pharmacological inhibition of soluble epoxide hydrolase on cardiac fibrosis. PLoS One. 2014; 9:e94092. [PubMed: 24718617]
19. Aharinejad S, Krenn K, Paulus P, Schäfer R, Zuckermann A, Grimm M, Abraham D. Differential role of TGF-beta1/bFGF and ET-1 in graft fibrosis in heart failure patients. Am J Transplant. 2005; 5:2185–2192. [PubMed: 16095497]
20. Hanna N, Cardin S, Leung TK, Nattel S. Differences in atrial versus ventricular remodeling in dogs with ventricular tachypacing-induced congestive heart failure. Cardiovasc Res. 2004; 63:236–244. [PubMed: 15249181]
21. Burstein B, Libby E, Calderone A, Nattel S. Differential behaviors of atrial versus ventricular fibroblasts: a potential role for platelet-derived growth factor in atrial-ventricular remodeling differences. Circulation. 2008; 117:1630–1641. [PubMed: 18347210]
22. Levine B, Kalman J, Mayer L, Fillit HM, Packer M. Elevated circulating levels of tumor necrosis factor in severe chronic heart failure. N Engl J Med. 1990; 323:236–241. [PubMed: 2195340]
23. Rahmutula D, Marcus GM, Wilson EE, Ding CH, Xiao Y, Paquet AC, Barbeau R, Barczak AJ, Erle DJ, Olgin JE. Molecular basis of selective atrial fibrosis due to overexpression of transforming growth factor-β1. Cardiovasc Res. 2013; 99:769–779. [PubMed: 23612580]
24. Kupfahl C, Pink D, Friedrich K, Zurbrügg HR, Neuss M, Warnecke C, Fielitz J, Graf K, Fleck E, Regitz-Zagrosek V. Angiotensin II directly increases transforming growth factor beta1 and osteopontin and indirectly affects collagen mRNA expression in the human heart. Cardiovasc Res. 2000; 46:463–475. [PubMed: 10912457]
25. Dobaczewski M, Chen W, Frangogiannis NG. Transforming growth factor (TGF)-β signaling in cardiac remodeling. J Mol Cell Cardiol. 2011; 51:600–606. [PubMed: 21059352]
26. Bjørnstad JL, Skrbic B, Marstein HS, Hasic A, Sjaastad I, Louch WE, Florholmen G, Christensen G, Tønnessen T. Inhibition of SMAD2 phosphorylation preserves cardiac function during pressure overload. Cardiovasc Res. 2012; 93:100–110. [PubMed: 22049534]
27. Jalife J, Kaur K. Atrial remodeling, fibrosis, and atrial fibrillation. Trends Cardiovasc Med. 2015; 25:475–484. [PubMed: 25661032]
28. Sovari AA, Dudley SC Jr. Reactive oxygen species-targeted therapeutic interventions for atrial fibrillation. Front Physiol. 2012; 3:311. [PubMed: 22934062]
29. Kamakura T, Makiyama T, Sasaki K, Yoshida Y, Wuriyanghai Y, Chen J, Hattori T, Ohno S, Kita T, Horie M, Yamanaka S, Kimura T. Ultrastructural maturation of human-induced pluripotent stem cell-derived cardiomyocytes in a long-term culture. Circulation J. 2013; 77:1307–1314.
30. Park CS, Cha H, Kwon EJ, Sreenivasaiah PK, Kim do H. The chemical chaperone 4-phenylbutyric acid attenuates pressure-overload cardiac hypertrophy by alleviating endoplasmic reticulum stress. Biochem Biophys Res Commun. 2012; 421:578–584. [PubMed: 22525677]
31. Luo T, Kim JK, Chen B, Abdel-Latif A, Kitakaze M, Yan L. Attenuation of ER stress prevents post-infarction-induced cardiac rupture and remodeling by modulating both cardiac apoptosis and fibrosis. Chem Biol Interact. 2015; 225:90–98. [PubMed: 25450231]

32. Harris TR, Bettaieb A, Kodani S, Dong H, Myers R, Chiamvimonvat N, Haj FG, Hammock BD. Inhibition of soluble epoxide hydrolase attenuates hepatic fibrosis and endoplasmic reticulum stress induced by carbon tetrachloride in mice. Toxicol Appl Pharmacol. 2015; 286:102–111. [PubMed: 25827057]
33. Bettaieb A, Chahed S, Tabet G, Yang J, Morisseau C, Griffey S, Hammock BD, Haj FG. Effects of soluble epoxide hydrolase deficiency on acute pancreatitis in mice. PloS One. 2014; 9:e113019. [PubMed: 25402489]
34. Groenendyk J, Agellon LB, Michalak M. Coping with ER stress in the cardiovascular system. Annu Rev Physiol. 2013; 75:49–67. [PubMed: 23020580]
35. Olsen NT, Dimaano VL, Fritz-Hansen T, Sogaard P, Chakir K, Eskesen K, Steenbergen C, Kass DA, Abraham TP. Hypertrophy signaling pathways in experimental chronic aortic regurgitation. J Cardiovasc Transl Res. 2013; 6:852–860. [PubMed: 23888404]
36. Ripplinger CM, Lou Q, Li W, Hadley J, Efimov IR. Panoramic imaging reveals basic mechanisms of induction and termination of ventricular tachycardia in rabbit heart with chronic infarction: implications for low-voltage cardioversion. Heart Rhythm. 2009; 6:87–97. [PubMed: 18996057]
37. Kistler PM, Sanders P, Dodic M, Spence SJ, Samuel CS, Zhao C, Charles JA, Edwards GA, Kalman JM. Atrial electrical and structural abnormalities in an ovine model of chronic blood pressure elevation after prenatal corticosteroid exposure: implications for development of atrial fibrillation. Eur Heart J. 2006; 27:3045–3056. [PubMed: 17098760]
38. Castillero E, Akashi H, Pendrak K, Yerebakan H, Najjar M, Wang C, Naka Y, Mancini D, Sweeney HL, D Armiento J, Ali ZA, Schulze PC, George I. Attenuation of the unfolded protein response and endoplasmic reticulum stress after mechanical unloading in dilated cardiomyopathy. Am J Physiol Heart Circ Physiol. 2015; 309:H459–470. [PubMed: 26055788]
39. Zhang W, Elimban V, Nijjar MS, Gupta SK, Dhalla NS. Role of mitogen-activated protein kinase in cardiac hypertrophy and heart failure. Exp Clin Cardiol. 2003; 8:173–183. [PubMed: 19649217]
40. Wakili R, Voigt N, Kääb S, Dobrev D, Nattel S. Recent advances in the molecular pathophysiology of atrial fibrillation. J Clin Invest. 2011; 121:2955–2968. [PubMed: 21804195]
41. Brandt MC, Priebe L, Böhle T, Südkamp M, Beuckelmann DJ. The ultrarapid and the transient outward K+ current in human atrial fibrillation. Their possible role in postoperative atrial fibrillation. J Mol Cell Cardiol. 2000; 32:1885–1896. [PubMed: 11013132]
42. Panama BK, Latour-Villamil D, Farman GP, Zhao D, Bolz SS, Kirshenbaum LA, Backx PH. Nuclear factor kappaB downregulates the transient outward potassium current I(to,f) through control of KChIP2 expression. Circ Res. 2011; 108:537–543. [PubMed: 21252158]
43. Sinnecker D, Goedel A, Laugwitz KL, Moretti A. Induced pluripotent stem cell-derived cardiomyocytes: a versatile tool for arrhythmia research. Circ Res. 2013; 112:961–968. [PubMed: 23569105]

WHAT IS KNOWN

- Atrial fibrillation (AF) represents the most common arrhythmia leading to increased morbidity and mortality, yet, current treatment strategies have proven inadequate.
- The soluble epoxide hydrolase enzyme (sEH) catalyzes the hydrolysis of anti-inflammatory epoxy fatty acids including epoxyeicosatrienoic acids from arachidonic acid to the corresponding diols.

WHAT THE STUDY ADDS

- Inhibition of sEH reduces inflammation, oxidative stress, fibrosis, and electrical remodeling. Mechanistically, treatment with sEH inhibitor significantly reduces the activation of key inflammatory signaling molecules, including the transcription factor nuclear factor κ-light-chain-enhancer (NF-κB), mitogen-activated protein kinase (MAPK) and transforming growth factor-β (TGF-β).
- This study provides insights into the underlying molecular mechanisms leading to AF by inflammation and represents a paradigm shift from conventional antiarrhythmic drugs which block downstream events to a novel upstream therapeutic target by counteracting the inflammatory processes in AF.

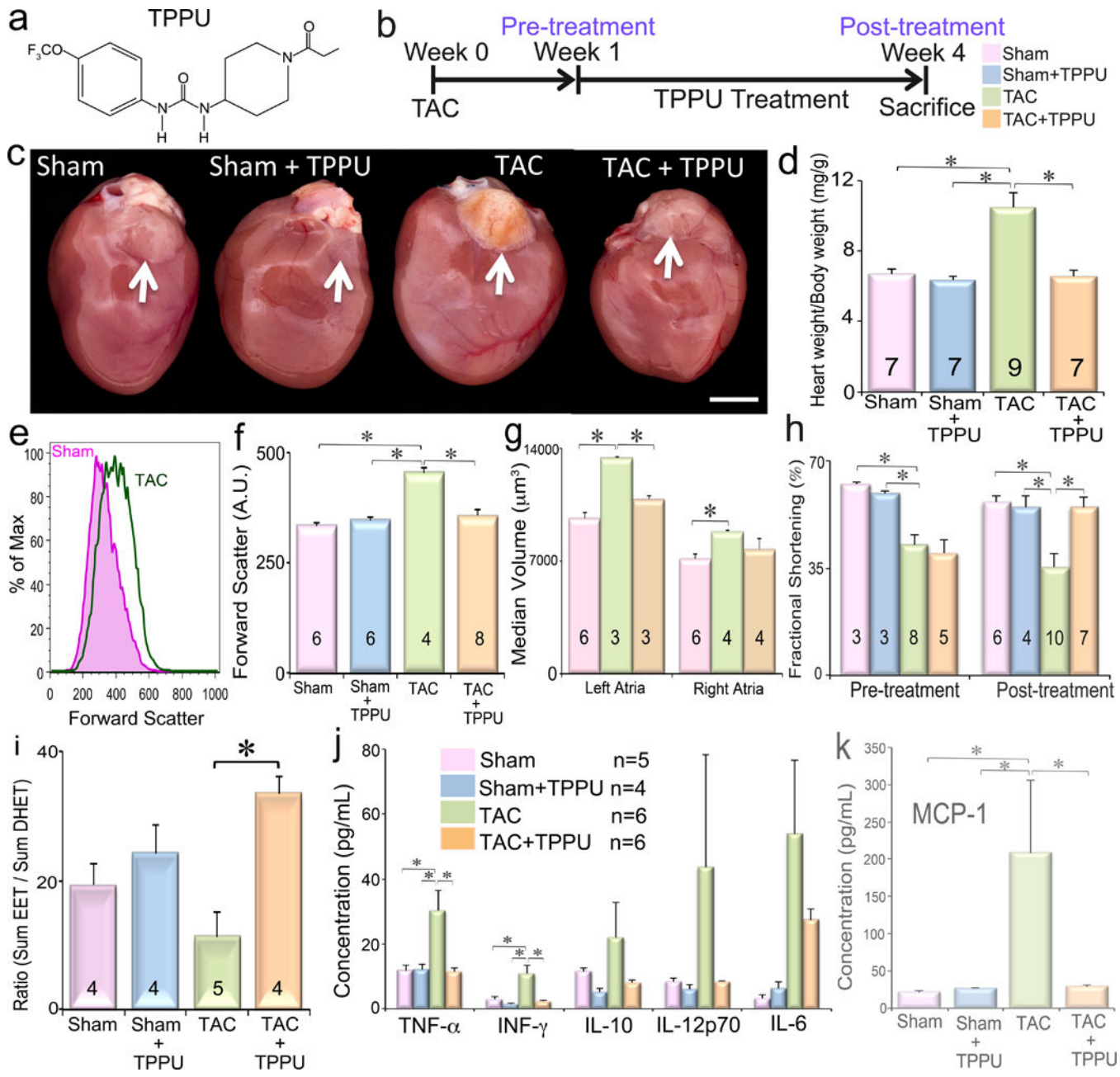

Figure 1.

TPPU prevents the development of atrial fibrosis in a murine Thoracic aortic constriction (TAC): **(a)** Structure of the sEHI, 1-trifluoromethoxyphenyl-3-(1-propionylpiperidine-4-yl) urea (TPPU) used in our studies. **(b)** Schematic representation of the experimental protocol. **(c)** Examples of whole hearts showing evidence of atrial dilatation in TAC mice. Scale=1 cm. **(d)** Summary data for heart weight/body weight (mg/g). **(e)** Flow cytometric analysis of isolated single nucleated atrial cardiomyocytes (cTnT-positive). **(f)** Summary data from (**e**). **(g)** Atrial myocyte volume measurements by the Coulter Multisizer assay. **(h)** Summary data for % fractional shortening. **(i)** Oxylipin profiling at 3 wk of follow-up. **(j)** Serum

concentration of cytokines and chemokine **(k).** Scale bars=20 μm. Mean±SEM, Numbers inside the graph represents n. **P<0.05.*

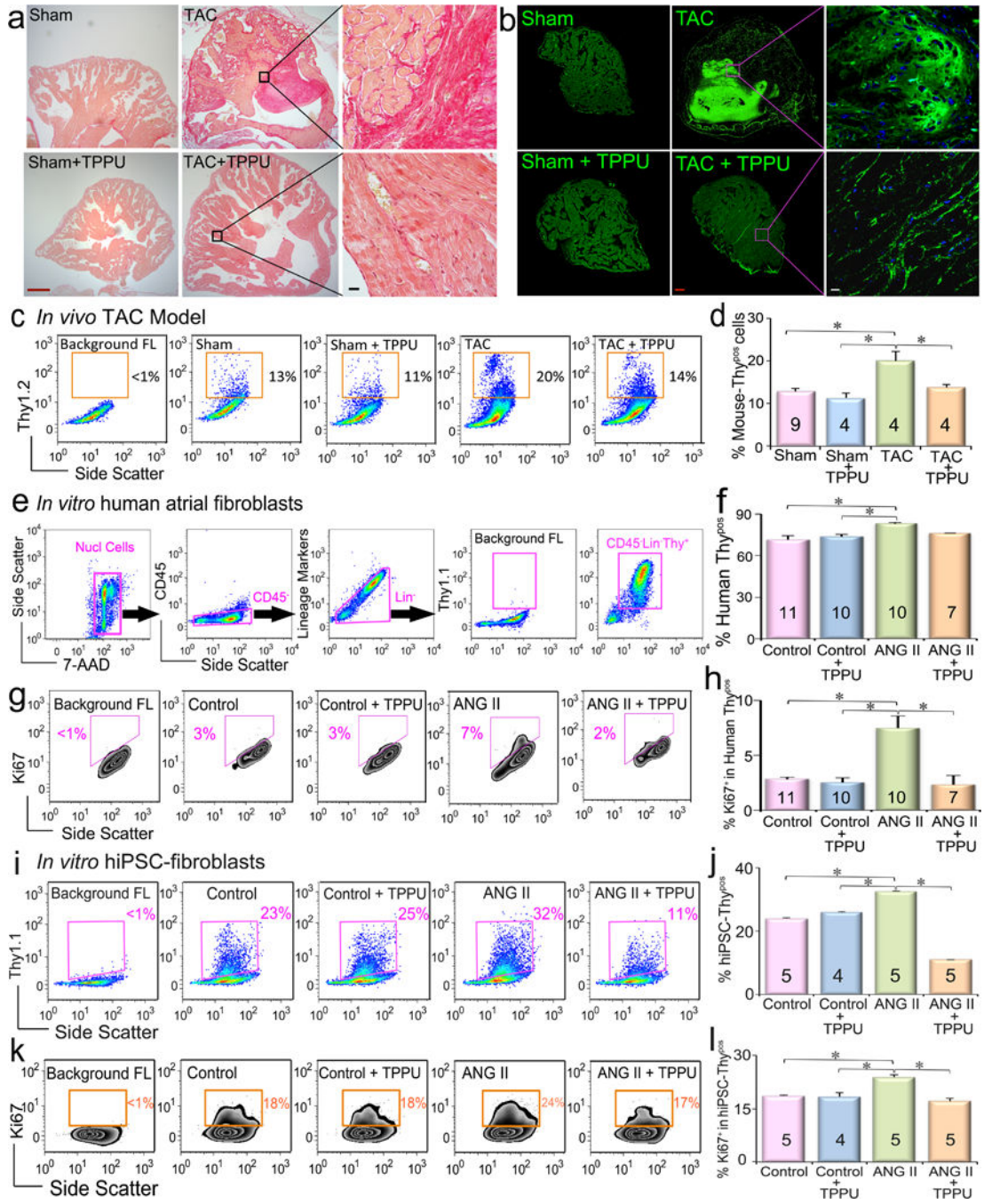

Figure 2.

TPPU reduces atrial fibrosis and atrial fibroblast activation: **(a)** Cardiac sections stained with Sirius Red demonstrate the amount of collagen deposition. Scale bars; red=500 μm and black=20 μm. **(b)** Confocal images of wheat germ agglutinin stain showing a significant decrease in collagen deposition in the TPPU-treated TAC mice compared to TAC alone. Scale bars; red=200 μm and white=20 μm **(c)** Flow cytometric analysis of $Thy1.2^{+}/Lin^{-}/CD31^{-}/CD45^{-}/CD34^{-}$ (Thy^{pos}) cells. X and Y-axes represent arbitrary units. **(d)** Summary data from (c). **(e)** Nucleated cells were enumerated based on the incorporation of 7-

aminoactinomycin D (7-AAD) from human atrial fibroblasts derived from human atrial appendage specimens from patients undergoing cardiac bypass surgery. Human atrial fibroblasts were identified as $Thy1.1^{+}/CD45^{-}/Lin^{-}$ (Human-Thy^{pos}) cells. **(f)** Flow cytometric analysis of human-Thy^{pos} cells. (**g**) Flow cytometric analysis of the proliferation of human-Thy^{pos} using Ki67. **(h)** Summary data from (g). **(i)** Flow cytometric analysis of $Thy1.1^{+}/CD45^{-}/Lin^{-}$ (hiPSC-Thy^{pos}) cells derived from hiPSCs. **(j)** Summary data from (i). (**k**) Flow cytometric analysis of the proliferation of hiPSC-Thy^{pos} cells using Ki67. **(l)** Summary data from (k). Representative results are shown. FL=fluorescence. Mean±SEM. Numbers inside the graph represents n. **P<0.05.*

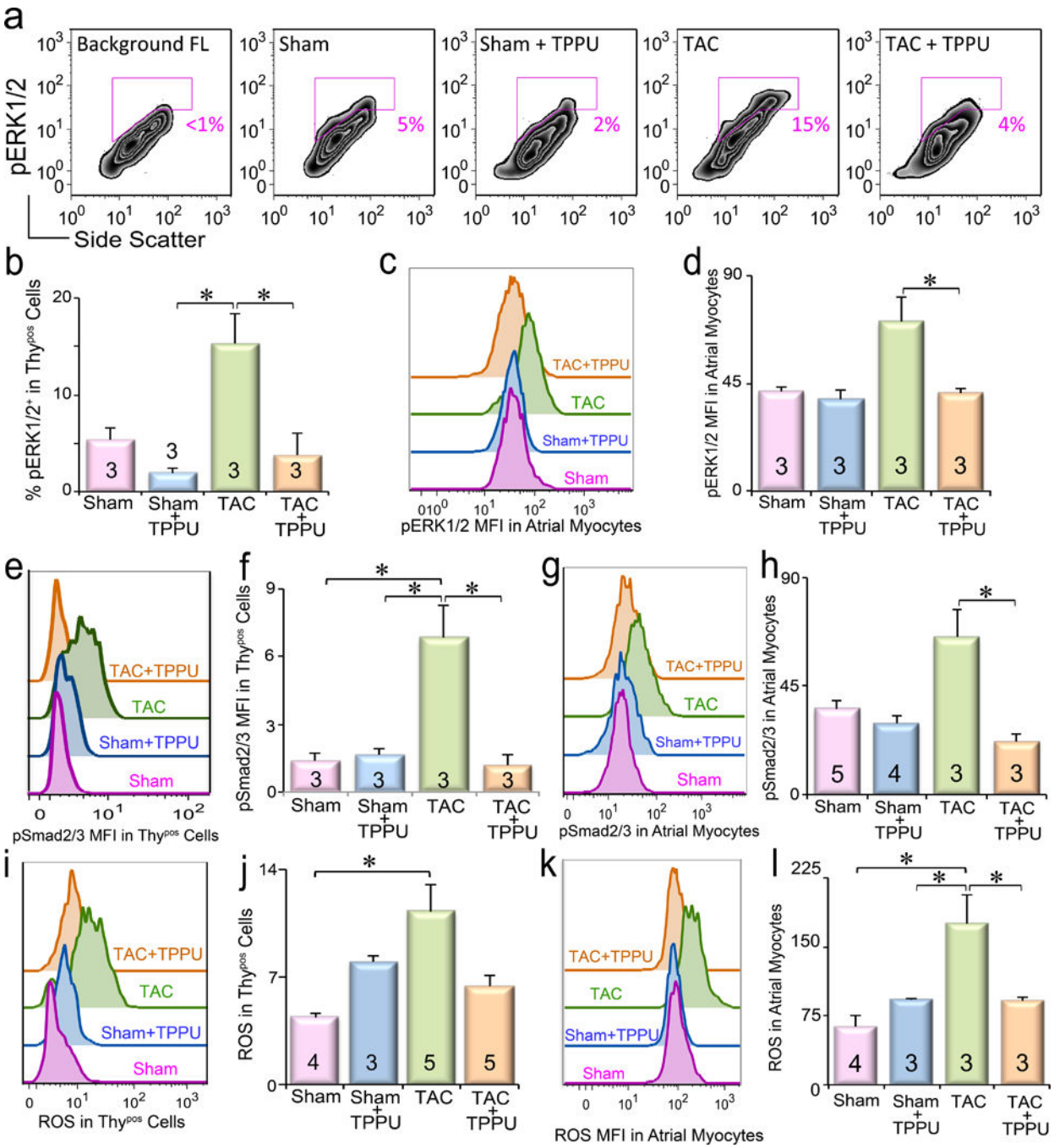

Figure 3.

Flow cytometric analysis of the activation of atrial cardiac fibroblasts and atrial myocytes in the in vivo TAC model: **(a)** Flow cytometric analysis of pERK1/2^{+} of atrial fibroblasts. **(b)** Summary data from (**a**). **(c)** Flow cytometric analysis showing the median fluorescence intensity of pERK1/2^{+} of atrial myocytes. **(d)** Summary data from (c). **(e)** Flow cytometric analysis of pSmad2/3^{+} in atrial fibroblasts. **(f)** Summary data from (**e**). **(g)** Flow cytometric analysis of pSmad2/3^{+} of atrial myocytes. **(h)** Summary data from (g). **(i)** Flow cytometric analysis of reactive oxygen species (ROS) of atrial fibroblasts. **(j)** Summary data from (**i**).

(k) Flow cytometric analysis of reactive oxygen species (ROS) of atrial fibroblasts. **(l)** Summary data from (**k**). Representative results are shown. Mean±SEM. Numbers inside the graph represent n. *$P<0.05$.

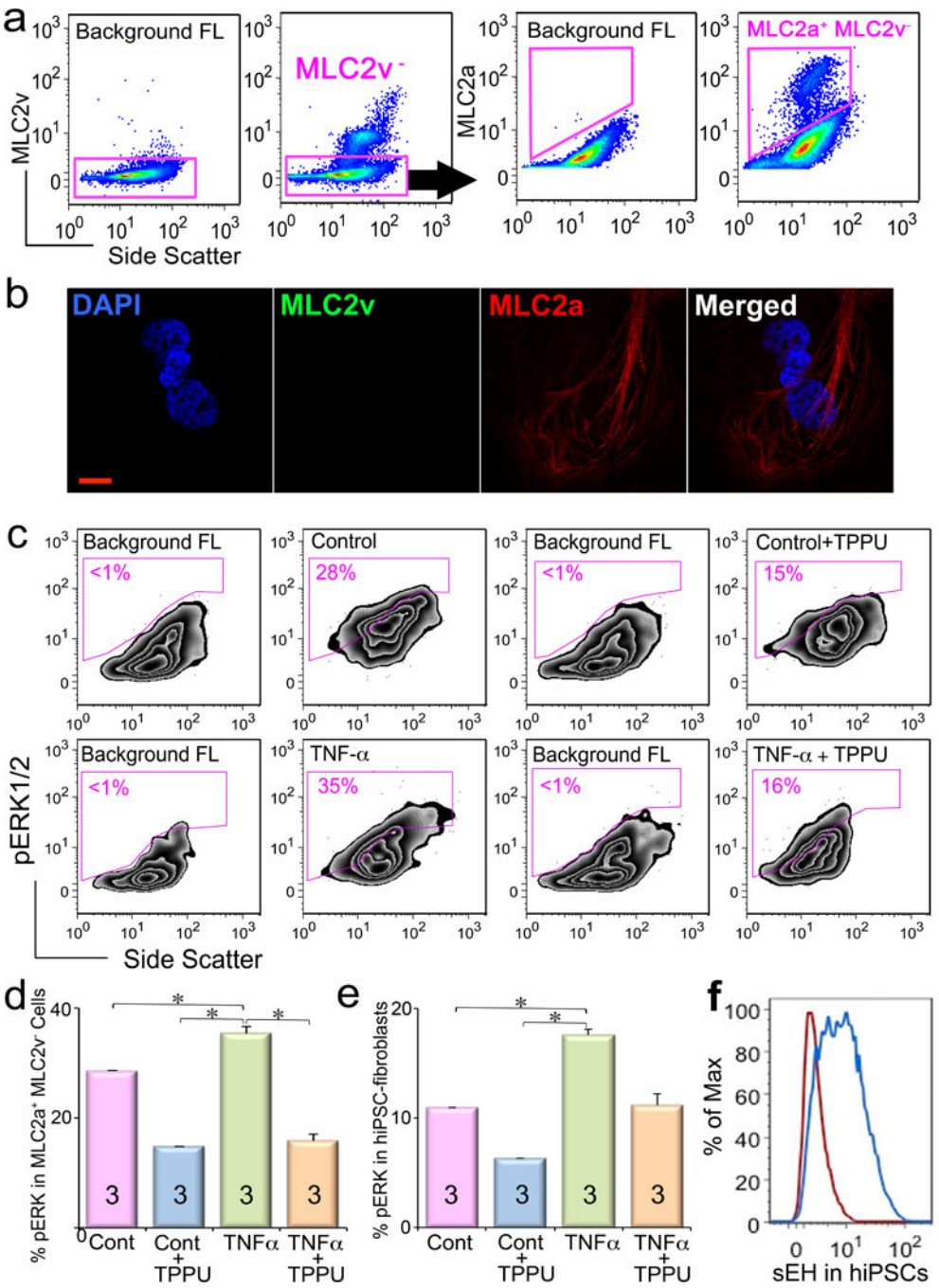

Figure 4.

Treatment with TPPU results in a significant reduction in ERK1/2 in atrial myocytes and fibroblasts in vitro: **(a)** Flow cytometric analysis of $MLC2a^{+}MLC2v^{-}$ cells from hiPSC-derived cardiomyocytes. X and Y-axes represent arbitrary units. **(b)** Immunofluorescence confocal images of $MLC2a^{+}MLC2v^{-}$ cells. **(c)** Flow cytometric analysis of pERK1/2 signal in $MLC2a^{+}MLC2v^{-}$ atrial myocytes treated with TNF-α alone and with TPPU. **(d)** Summary data from (c). **(e)** Flow cytometric summary data showing pERK1/2 signal in hiPSC-fibroblasts ($Thy1.1^{+}/CD45^{-}/Lin^{-}$) treated with TNF-α alone and with TPPU. **(f)**

Presence of sEH in hiPSCs analyzed through flow cytometry. Scale bar = 200 μM. Mean ±SEM. Numbers inside the graph represent n. **P<0.05.*

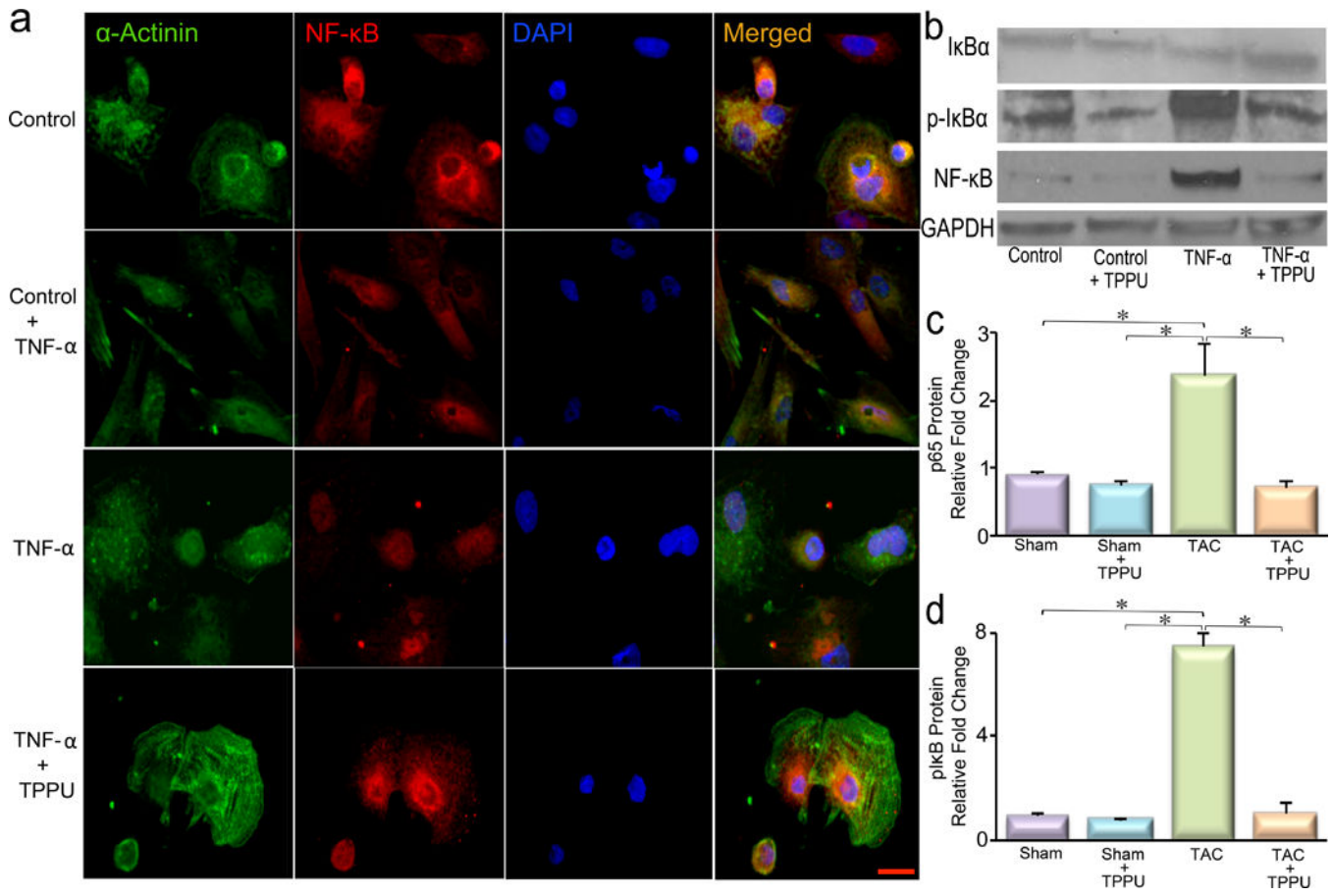

Figure 5.

Treatment with TPPU results in NF-κB activation hiPSC-CMs in vitro: **(a)** Prevention of translocation of NF-κB after treatment with TPPU in cultured hiPSC-CMs stimulated with TNF-α. **(b)** Western blot analysis of total IκBα, phosphorylated IκBα (pIκBα), nuclear NF-κB (nNF-κB) and GAPDH levels. **(c)** Quantification of nuclear NF-κB and **(d)** pIκBα normalized to GAPDH. Mean±SEM. n=3. **P<0.05*

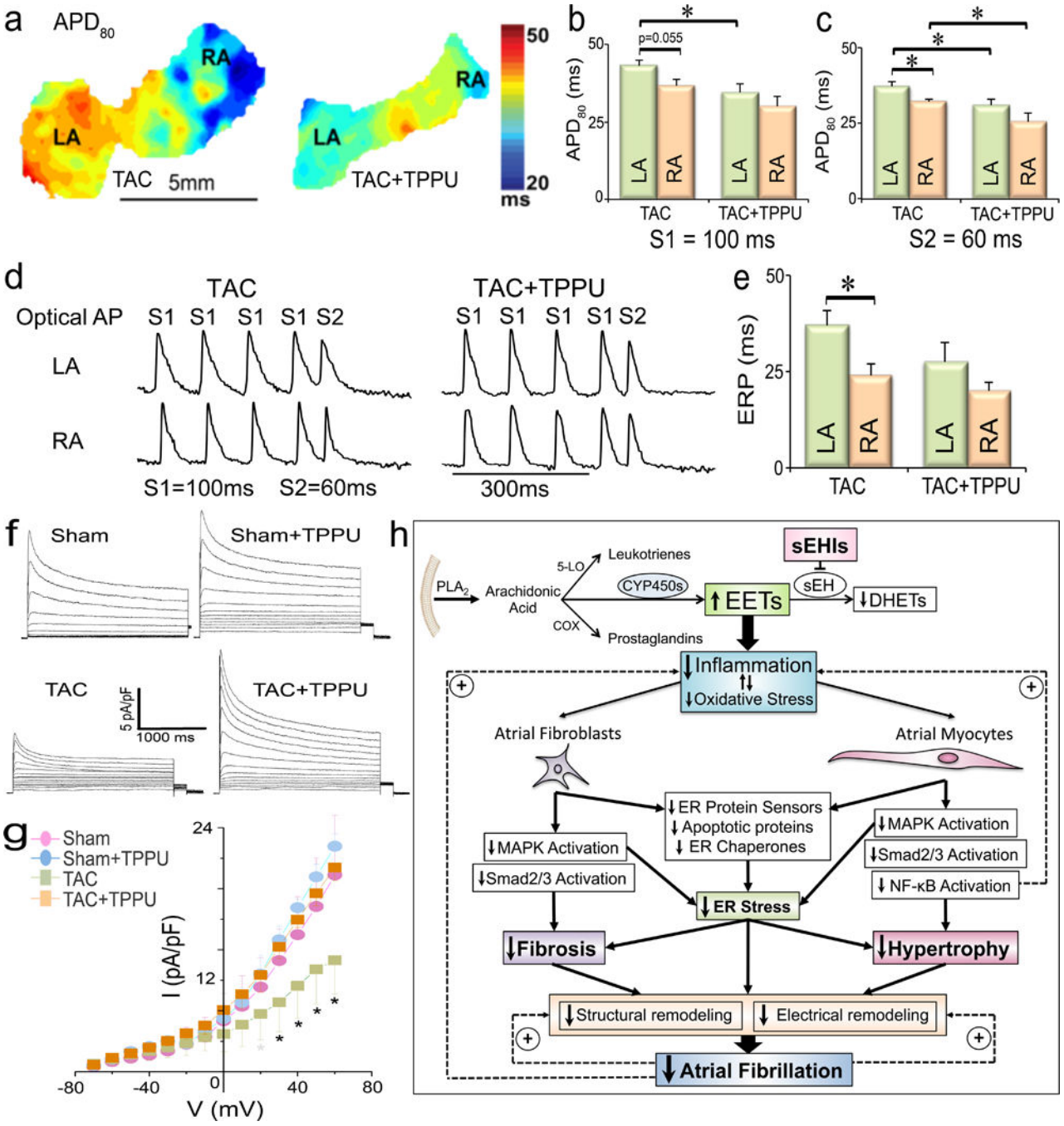

Figure 6.

Effect of TPPU on TAC-induced atrial electrophysiological remodeling: **(a)** Example maps of atrial action potential duration (APD) in the untreated (left) and TPPU-treated (right) heart. **(b)** Example optical AP traces during S1 (100 ms)-S2 (60 ms). **(c)** Mean APD_{80} during pacing at a constant cycle length (S1=100 ms). **(c)** Mean APD_{80} during a premature pacing stimulus (S2=60 ms). **(d)** Example optical AP traces during S1 (100ms)-S2 (60ms) pacing. **(e)** Effective refractory period (ERP) measured from both the LA and RA in untreated and TPPU-treated hearts. n=5 in TAC, n=4 in TAC+TPPU. **(f)** Transient outward

K^+ current recordings from single isolated atrial myocytes and **(g)** the corresponding current-voltage (I-V) plot. Representative results are shown. (h) Summary of the various processes involved in the prevention of AF with TPPU treatment. Mean±SEM, n=14. **P<0.05.*